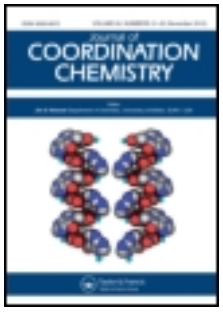

Journal of Coordination Chemistry
Publication details, including instructions for authors and subscription information:
http://www.tandfonline.com/loi/gcoo20

Sonochemical synthesis of a novel nanorod diaqua(pyridine-2,6-dicarboxylato)copper(II) 3-D supramolecular network: new precursor to prepare pure phase nanosized copper(II) oxide

Rimpy Gupta [a], Sumit Sanotra [a], Haq Nawaz Sheikh [a], Bansi Lal Kalsotra [a], Vivek Kumar Gupta [b] & Rajnikant [b]

[a] Department of Chemistry, University of Jammu, Jammu-180006, India

[b] Department of Physics, University of Jammu, Jammu-180006, India

Accepted author version posted online: 11 Sep 2012.Published online: 26 Sep 2012.

To cite this article: Rimpy Gupta, Sumit Sanotra, Haq Nawaz Sheikh, Bansi Lal Kalsotra, Vivek Kumar Gupta & Rajnikant (2012) Sonochemical synthesis of a novel nanorod diaqua(pyridine-2,6-dicarboxylato)copper(II) 3-D supramolecular network: new precursor to prepare pure phase nanosized copper(II) oxide, Journal of Coordination Chemistry, 65:22, 3917-3931, DOI: 10.1080/00958972.2012.728592

To link to this article: http://dx.doi.org/10.1080/00958972.2012.728592

Journal of Coordination Chemistry
Vol. 65, No. 22, 20 November 2012, 3917–3931

Sonochemical synthesis of a novel nanorod diaqua(pyridine-2, 6-dicarboxylato)copper(II) 3-D supramolecular network: new precursor to prepare pure phase nanosized copper(II) oxide

RIMPY GUPTA†, SUMIT SANOTRA†, HAQ NAWAZ SHEIKH*†, BANSI LAL KALSOTRA†, VIVEK KUMAR GUPTA‡ and RAJNIKANT‡

†Department of Chemistry, University of Jammu, Jammu-1800 06, India
‡Department of Physics, University of Jammu, Jammu-1800 06, India

(*Received 11 June 2012; in final form 23 July 2012*)

A nanosized copper(II) supramolecular compound, $[Cu(dipic)(H_2O)_2]_n$ (**1**) [dipic = 2, 6-pyridinedicarboxylate], has been synthesized by sonochemical method and characterized by elemental analysis, scanning electron microscopy, X-ray powder diffraction, IR spectroscopy, TGA/DTA, and BET surface area studies. The structure of single crystalline **1** developed from nanosized **1** has been determined by X-ray crystallography and further characterized by scanning electron microscopy, TGA/DTA, and BET surface area studies. The XRD studies reveal that nanorod copper(II) supramolecular compound adopts a 3-D supramolecular network owing to extensive hydrogen-bonding and π–π stacking. Solvent effects on size and morphology of nanosized **1** have been studied. Calcination of nanosized **1** at 500°C under air yields CuO nanoparticles.

Keywords: Sonochemical; Supramolecular; BET surface area; Nanoparticles

1. Introduction

Considerable progress has been made on crystal engineering of supramolecular architectures organized and sustained by coordinate covalent bonds, supramolecular contacts (such as hydrogen bonds and π–π interaction), nucleophilic interaction, etc. [1–3]. Organic and metal–organic materials that exhibit micro- and nanoporous behavior have been reported with crystalline structures that are stable upon removal of guest molecules [4–8]. Such porous materials have potential for commercial application in areas such as molecular separations, catalysis, storage, photonic materials, and synthetic zeolites [9]. Molecular building blocks with multiple sites for hydrogen-bonding or metal–ligand coordination frequently form multiple frameworks that have different structures or intermolecular connectivity [10]. This approach to crystal engineering uses metal–ligand bonds between transition metals and organic ligands to create coordination polymers that have extended structures [1, 11–17]. 2,6-Pyridinedicarboxylic acid (H_2dipic) has three coordinating sites. Polymeric

*Corresponding author. Email: hnsheikh@rediffmail.com

ISSN 0095-8972 print/ISSN 1029-0389 online © 2012 Taylor & Francis
http://dx.doi.org/10.1080/00958972.2012.728592

structures of 2,6-pyridinedicarboxylato complexes with transition and lanthanide metals have been reported, in which 2,6-pyridinedicarboxylate not only chelates but also bridges to form diversified structures [18–24].

The size and shape of solid materials influence chemical and physical properties. By decreasing the size of coordination supramolecular polymers to nanosize, surface area would be increased, resulting in change in physical and chemical properties [25–28]. Nanostructured materials have been prepared by various synthetic methods, including gas phase techniques, liquid phase methods, and mixed phase approaches [29–31]. In sonochemistry, molecules undergo a chemical reaction due to the application of powerful ultrasound irradiation (20 kHz–10 MHz). Ultrasound induces chemical changes due to cavitation phenomena involving formation, growth, and instantaneously implosive collapse of bubbles in a liquid, which can generate local hot spots having a temperature of roughly 5000°C, pressures of about 500 atm and a lifetime of a few microseconds [32]. These extreme conditions can drive chemical reactions to fabricate a variety of nanocompounds [33, 34]. Bang and Suslick have used ultrasound to synthesize nanostructured materials of diverse composition and morphology [31, 35, 36]. So far little attention has been given to synthesis of nanosized supramolecular compounds.

In this article, we report a new molecular building block of Cu^{2+} with H_2dipic by incorporating additional hydrogen-bonding functionality on 2,6-pyridinedicarboxylate. The new building block promotes formation of a layered framework. The additional hydrogen-bonding groups on the pyridyl ring promote stacking of the 2-D framework and provide control in three dimensions over the spacing and alignment of pores between adjacent layers. Crystalline materials grown using this strategy can trap molecules of solvent in channels that are aligned in parallel. We also describe a simple sonochemical preparation of nanostructures of $[Cu(dipic)(H_2O)_2]_n$ (**1**) and its use as a precursor for the preparation of CuO nanoparticles.

2. Experimental

2.1. *Materials and methods*

All reagents used for the synthesis and analysis were commercially available and used as received. Doubly distilled water was used to prepare aqueous solutions. An ultrasonic processer with thumb-actuated pulser (Sonics make) equipped with a standard probe made of titanium alloy Ti-6 Al-4V operating at 20 kHz with a maximum power output of 130 W was used for the ultrasonic irradiation. The melting points (uncorrected) were determined on an Electrothermal 9200 Barnstead. Microanalyses were carried out using a CHNS analyzer Leco Model-932. IR spectra from 4000 to 400 cm^{-1} were recorded on a Perkin-Elmer Model-Spectrum RX 1 FTIR spectrophotometer using KBr discs. Thermal analysis was performed on a Perkin-Elmer (Pyris Diamond) TG-7 thermo-analyser under static air at heating rate of 10°C min^{-1}. The simulated X-ray powder diffraction (XRPD) pattern based on single-crystal data was prepared using Mercury software [37]. XRPD measurements were performed using a Bruker AXSD8 X-ray diffraction spectrometer with monochromated Cu-Kα radiation and SEM using Jeol make T-300 scanning electron microscope with gold coating. Particle size was determined by the dynamic light scattering (DLS) technique using a Zetasizer Nano ZS 90, Malvern make.

2.2. *Synthesis of [Cu(dipic)(H$_2$O)$_2$]$_n$ (1) nanostructure by a sonochemical process*

To prepare nanosized [Cu(dipic)(H$_2$O)$_2$]$_n$ (**1**), a 50 mL aqueous solution of copper nitrate trihydrate (1.812 g, 0.15 mol L^{-1}) was positioned in a high density ultrasonic probe. Into this solution, 50 mL aqueous solution of 2,6-pyridinedicarboxylic acid (0.836 g, 0.1 mol L^{-1}) and NaOH (0.4 g, 0.2 mol L^{-1}) were added dropwise. The reaction was carried out at room temperature. Blue precipitates were formed after aging 1 h. The precipitates formed were filtered off, washed with water, and dried in air. Yield: 82%; m.p.: >300°C. Elemental Anal. Calcd for $C_7H_7CuNO_6$ (%): C, 31.82; H, 2.70; N, 5.31. Found (%): C, 31.76; H, 2.66; N, 5.29.

For study of solvent effect on size and morphology of **1** the above process was also done with water/methanol solvent. The calcination of nanosized **1** at 500°C in a furnace and static atmosphere of air for 5 h produced CuO nanoparticles.

2.3. *Synthesis of single crystals of [Cu(dipic)(H$_2$O)$_2$]$_n$ (1)*

In order to isolate singe crystals of [Cu(dipic)(H$_2$O)$_2$]$_n$ (**1**), the blue precipitates were dissolved in minimum distilled water in a beaker and left to evaporate. After 20 days, blue block-shaped crystals were formed, were washed with water, and dried in air. Yield: 35%; m.p.: >300°C. Elemental Anal. Calcd for $C_7H_7CuNO_6$ (%): C, 31.80; H, 2.71; N, 5.30. Found (%): C, 31.76; H, 2.66; N, 5.29.

2.4. *Crystal structure and refinement*

Single-crystal analysis of **1** was carried out. X-ray intensity data of 9240 reflections (of which 1490 were unique) were collected on an X'calibur CCD area-detector diffractometer equipped with graphite monochromated Mo-Kα radiation ($\lambda = 0.71073$ Å). The crystal used for data collection was $0.30 \times 0.20 \times 0.20$ mm. The cell dimensions were determined by least-squares fit of angular settings of 7995 reflections in the θ range of 3.98–28.94°. The intensities were measured by ω scan mode for θ range 4.31–25.00°. About 1442 reflections were treated as observed ($I > 2\sigma(I)$). Data were corrected for Lorentz, polarization, and absorption factors. The structure was solved by direct methods using SHELXS97. All non-hydrogen atoms were located in the best *E*-map. Full-matrix least-squares refinement was carried out using SHELXL97. The final refinement cycles converged to $R = 0.0221$ and $wR(F^2) = 0.0589$ for the observed data. Residual electron densities ranged from -0.286 to $0.279\,e\,Å^{-3}$. Atomic scattering factors were taken from International Tables for X-ray Crystallography (1992, Vol. C, Tables 4.2.6.8 and 6.1.1.4). The crystallographic data are summarized in table 1.

2.5. *N_2 TPD and BET surface area*

N_2 adsorption/desorption isotherms and BET surface area were determined on a CHEMBET-3000 (TPR/TPD/TPO) instrument containing a quartz reactor (i.d = 4 mm) and a TCD detector. Prior to N_2 adsorption, samples were pre-treated in helium gas at 300°C for 2 h to remove any adsorbed impurities. Subsequently, the samples were cooled to room temperature in helium gas flow. The adsorption of N_2 was carried out by passing a mixture of 10% N_2 balanced helium gas over the samples for 1 h. Finally, the system

Table 1. Crystal data and structure refinement data for **1**.

CCDC No.	849605
Crystal description	Block-shaped
Crystal color	Blue
Crystal size (mm^3)	$0.30 \times 0.20 \times 0.20$
Empirical formula	$C_7H_7CuNO_6$
Formula weight	264.68
Radiation, wavelength (Å)	Mo-Kα, 0.71073
Unit cell dimensions (Å, °)	
a	4.7239(2)
b	8.9845(4)
c	10.3454(4)
α	81.132(4)
β	85.697(4)
γ	83.312(4)
Crystal system	Triclinic
Space group	$P-1$
Unit cell volume	430.15(3)
No. molecules per unit cell, Z	2
Temperature (K)	293(2)
Absorption coefficient (mm^{-1})	2.548
$F(000)$	266
Scan mode	ω scan
θ range for entire data collection (°)	$4.31 < \theta < 25.00$
Range of indices	$-5 \le h \le 5$; $-10 \le k \le 10$; $-12 \le l \le 12$
Reflections collected/unique	9240/1490
Reflections observed ($I > 2\sigma(I)$)	1442
R_{int}	0.0300
R_{sigma}	0.0176
Structure determination	Direct methods
Refinement	Full-matrix least-squares on F^2
No. parameters refined	164
Final R	0.0221
wR (F^2)	0.0589
Weight	$1/[\sigma^2(F_o^2) + (0.0327\ P)^2 + 0.3913\ P]$, where $P = [F_o^2 + 2F_c^2]/3$
Goodness-of-fit	1.035
$(\Delta/\sigma)_{max}$	0.001 (U11 H61)
Final residual electron density (e $Å^{-3}$)	$-0.286 < \Delta\rho < 0.279$
Measurement	X'calibur system – Oxford diffraction make, UK
Software for structure solution	SHELXS97 (Sheldrick, 1997)
Software for refinement	SHELXL97 (Sheldrick, 1997)
Software for molecular plotting	ORTEP-3 (Farrugia, 1997); PLATON (Spek, 2003)
Software for geometrical calculation	PLATON (Spek, 2003); PARST (Nardelli, 1995)

was heated from 80°C to 1200°C at 10°C min^{-1} and the desorbed gas was monitored with a TCD detector. All the flow rates were maintained at normal temperature and pressure (NTP).

3. Results and discussion

Reaction of 2,6-pyridinedicarboxylate with copper nitrate trihydrate leads to a 3-D supramolecular compound $[Cu(dipic)(H_2O)_2]_n$ (**1**). Nanoparticles of **1** were obtained

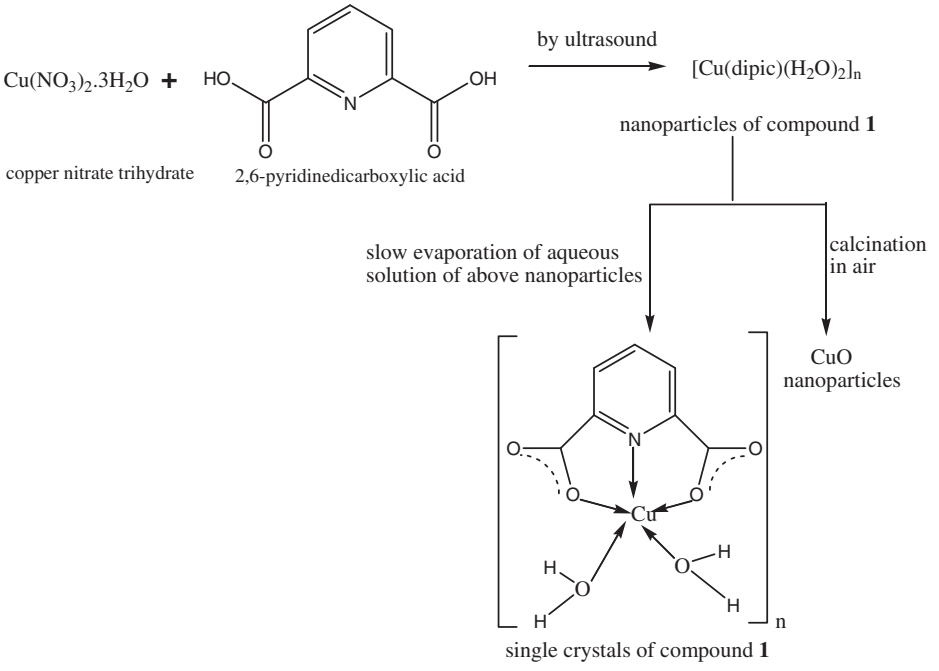

Scheme 1. Overview of the method for synthesis of $[Cu(dipic)(H_2O)_2]$.

both in purely aqueous solution and methanol:water, 1 : 1 by ultrasonic irradiation, while single crystals of **1** were obtained by slow evaporation of aqueous solution of the nanoparticles. Scheme 1 gives an overview of the method used for the synthesis of $[Cu(dipic)(H_2O)_2]_n$ (**1**). Further, nanosized **1** was calcined at 500°C in a furnace and static atmosphere of air for 5 h to produce nanoparticles of CuO.

3.1. *IR spectral studies*

The IR spectra of nanoparticles of **1** produced by sonochemical method and that of single crystals of **1** are indistinguishable (figure 1). The most salient feature of IR spectra of **1** is the existence of strong bands at 1681, 1657, and 1623 cm^{-1} attributed to $\nu(C=O)$ and at 1368 cm^{-1} attributed to $\nu(C–O)$. A weak band at 1597 cm^{-1} is assigned to $\nu(C=N)$. Weak bands at 605 and 445 cm^{-1} are attributed to Cu–N and Cu–O stretching vibrations, respectively. The broad band near 3480 cm^{-1} shows the existence of coordinated water [38, 39].

3.2. *XRPD diffraction studies*

The simulated XRPD pattern from single-crystal X-ray data of **1** in comparison with the XRPD pattern of a typical sample of **1** prepared by sonochemical process is shown in the Supplementary material section. Acceptable matches, with slight differences in 2θ, were observed between simulated and experimental XRPD patterns. This indicates that the compound obtained by the sonochemical process as nanoparticles is identical to

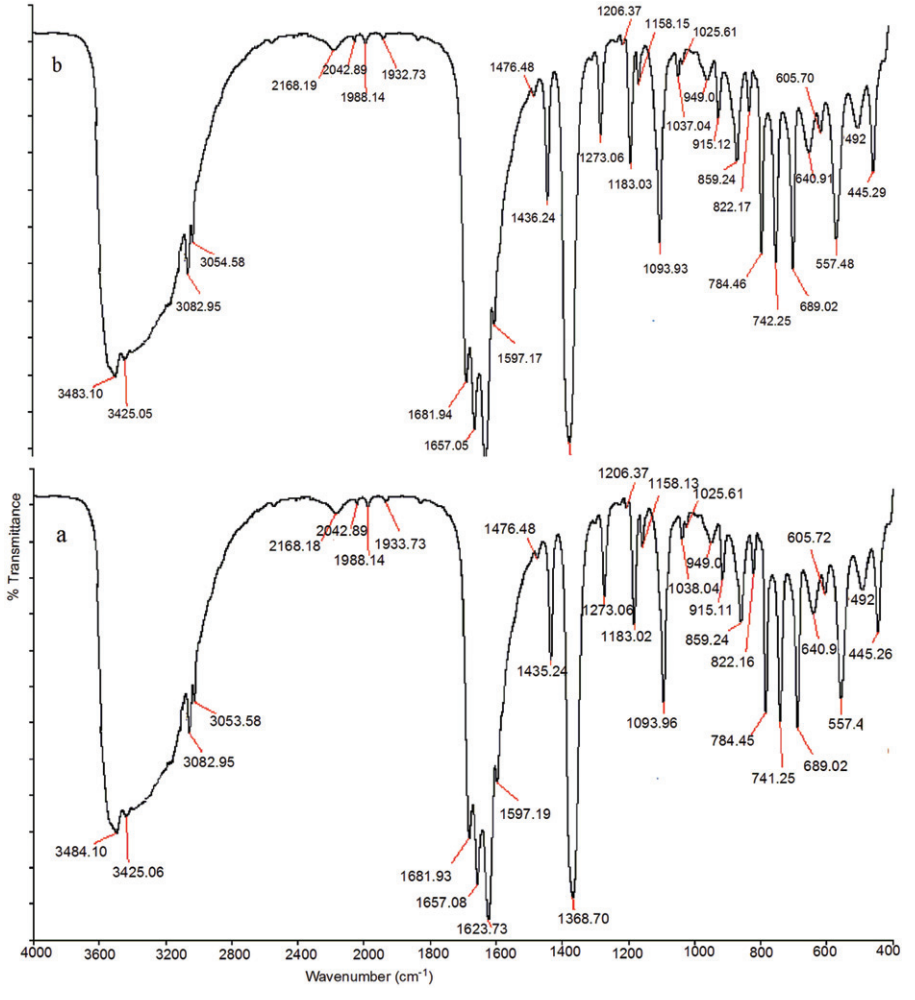

Figure 1. IR spectra of (a) single crystals of **1** and (b) nanoparticles of **1** produced by sonochemical method.

that obtained by single-crystal diffraction. Significant broadening of the peaks indicates that the particles obtained by sonochemical process are of nanometer dimensions.

Figure 2 shows the XRPD pattern of the residue obtained from calcination of nanoparticles of **1** at 500°C. All peaks in the diffraction diagram could be assigned to the monoclinic phase CuO with lattice parameters $a = 4.655$ Å, $b = 3.432$ Å, and $c = 5.126$ Å, which is also in agreement with standard data from JCPDS card no. 05-0661. No peaks of impurities are detected in the XRPD pattern, indicating the high purity of as-obtained sample. Sharp diffraction peaks indicate good crystallinity of CuO. The broad diffraction peaks indicate that the particles are of nanometer dimensions. By using Debye–Scherrer equation,

$$L = 0.89\lambda/\beta\cos\theta,$$

where L is the average crystallite size, $\lambda = 1.5418$ Å for Cu-Kα, β is the half maximum peak width, and θ is the diffraction angle in degrees, the average crystallite size was

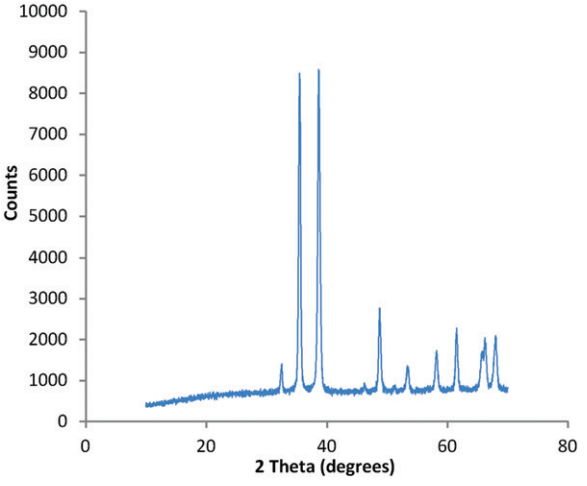

Figure 2. XRPD pattern of CuO nanoparticles prepared by calcination of nanosized **1** at 500°C.

found to be 20 nm. Nanoparticles of metal oxides have been obtained by calcination of metal–organic frameworks [40] and nanosized coordination polymers [41, 42]. In our study, nanoparticles of copper oxide were obtained by calcination of nanosized supramolecular compound $[Cu(dipic)(H_2O)_2]_n$ (**1**).

3.3. *SEM and DLS studies*

The SEM image of single crystals of **1** is shown in the Supplementary material section. The SEM image reveals that the single crystals have disc-like morphology with sharp edges. Figure 3(a) indicates the morphology of **1** prepared by sonochemical method in pure water. The morphology is composed of nanorods with sizes of about 350–384 nm. Figure 3(b) shows the morphology of **1** prepared by sonochemical method in methanol : water, 1 : 1. Particles obtained in mixed solvent (figure 3b) have large sizes and polyhedral morphology with well-defined faces. We further examined the particle size of nanosized **1** by DLS characterization. DLS measurements show mean particle size of 381 nm (figure 4a) for **1** prepared in water and 399 nm (figure 4b) for that prepared in water/methanol with narrow size distribution, in agreement with the data obtained from SEM images. Continuous sheet-like SEM image of CuO nanoparticles with well-defined pores are shown in the Supplementary material section.

The IR spectrum and XRPD pattern of a typical sample of **1** prepared by sonochemical process in mixed solvent system are also the same as those of the crystalline sample, showing that reaction in two different solvents produces the same compound but with different size and morphology.

3.4. *Single-crystal X-ray structure*

X-ray crystallographic study of **1** shows that the complex is a 3-D supramolecular framework. The coordination environment around copper(II) in **1** is shown in figure 5 and the packing arrangement of **1** viewed along different axes is shown in figure 6.

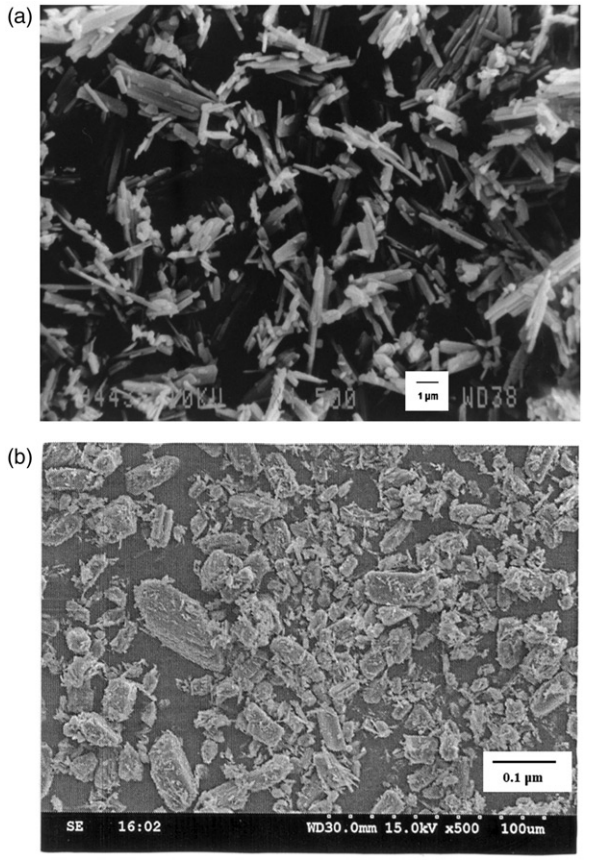

Figure 3. SEM images: (a) SEM image of nanoparticles of **1** produced in aqueous medium and (b) SEM image of nanoparticles of **1** produced in mixed solvents.

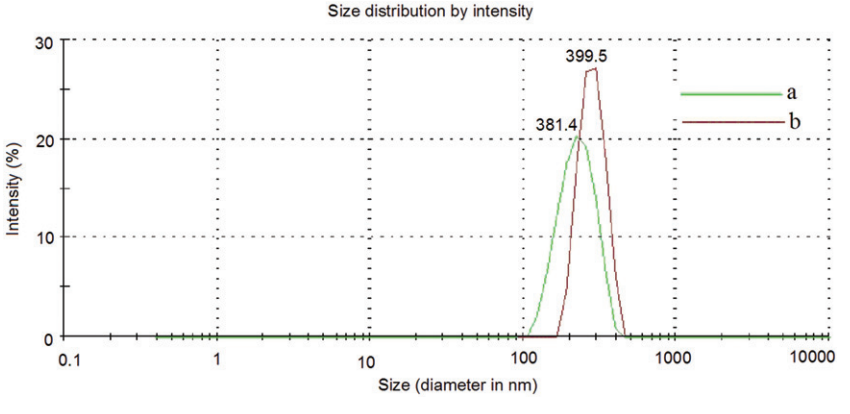

Figure 4. Particle size determination of (a) nanosized **1** produced in aqueous medium and (b) nanosized **1** produced in mixed solvents by the DLS technique.

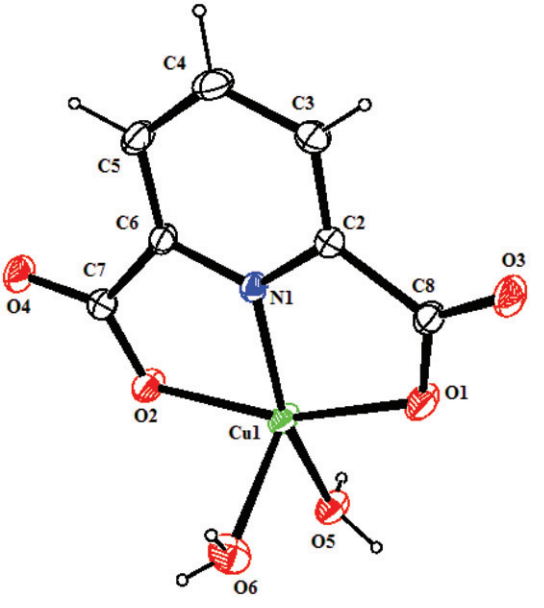

Figure 5. ORTEP diagram of **1**.

Complex **1** crystallizes in the triclinic space group with space group *P*-1. Relevant crystallographic data for **1** are listed in table 1. Table 2 lists selected bond distances and angles for **1**. Copper(II) is five-coordinate in a distorted square-pyramidal environment with a $CuNO_4$ core with two oxygen atoms [O(1), O(2)] and one nitrogen atom [N(1)] from dipic and two oxygen atoms [O(5), O(6)] from coordinated water molecules. Copper with dipic and O(5) are approximately in a plane. The apical site is occupied by O(6) which is weakly coordinated [Cu(1)–O(6) = 2.1564(19) Å] as in previous reports [43]. Distorted stereochemistry is to be expected for Cu(II) as a consequence of the non-spherical symmetry of the d^9 electronic configuration, ascribed to the Jahn–Teller effect with associated vibronic coupling [43]. The C–O distances [O(3)–C(8) = 1.235(3) Å, O(1)–C(8) = 1.278(3) Å, O(2)–C(7) = 1.285(3) Å and O(4)–C(7) = 1.224(3) Å] are generally shorter than other C–O distances, indicating conjugation of the double bond after deprotonation. Thus, the two oxygen atoms of carboxylates of 2,6-pyridinedicarboxylic acid after deprotonation contribute two negative charges. The crystal structure of the distorted octahedral complex bis(pyridine-2,6-dicarboxylato-N,O,O′)copper(II) monohydrate has been reported [44]. The copper(II) complex exhibits twofold crystallographic symmetry and contains two different ligand molecules, one neutral and the other doubly ionized.

Each uncoordinated carboxylate oxygen atom of **1** is hydrogen-bonded to the pyridine ring meta-hydrogen of one adjacent unit as well as to water of the other adjacent unit in the same layer. This leads to a symmetrical supramolecular structure (figure 7). Water molecules are involved in extensive hydrogen-bonding, showing intramolecular hydrogen-bonding with copper coordinated carboxylate oxygen atoms and intermolecular hydrogen-bonding with uncoordinated carboxylate oxygen atoms of adjacent units in the adjacent layers. One water molecule is further hydrogen-bonded to the copper coordinated carboxylate oxygen of the adjacent unit (figure 7). In this way,

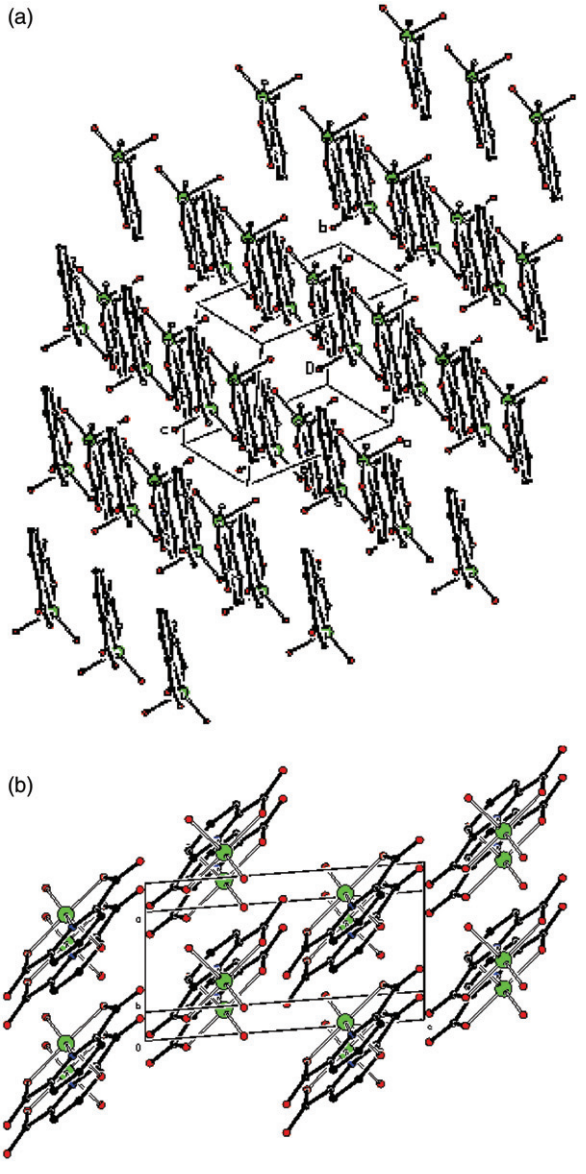

Figure 6. Packing arrangement of **1** when viewed along the (a) *a*-axis, (b) *b*-axis, and (c) *c*-axis.

each unit is hydrogen-bonded to four adjacent units, leading to symmetrical π–π stacking of the units in a supramolecular framework. Figure 8 shows the number and position of hydrogen bonds in the supramolecular framework. Table 3 lists hydrogen-bonding distances and angles for **1**.

3.5. *Thermal studies*

To examine the thermal stability of the nanorods and the single-crystalline material of **1**, the thermal decomposition behavior (TGA/DTA) was investigated in static air

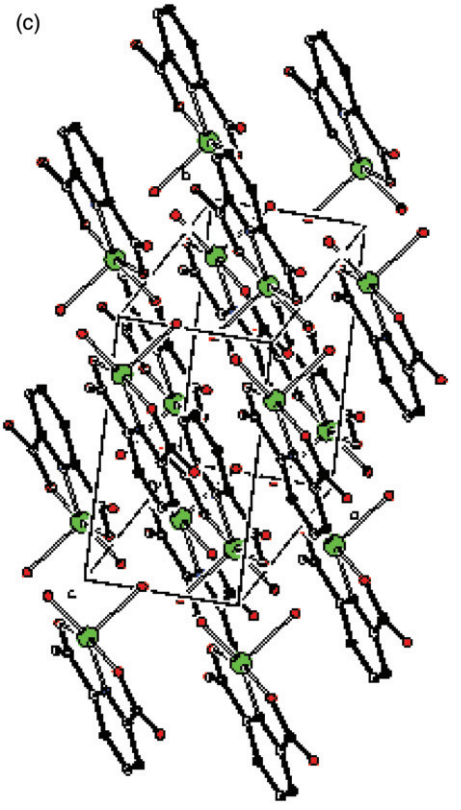

Figure 6. Continued.

from 30°C to 700°C. Single crystals of **1** and nanosized particles (Supplementary material) show similar behavior. Below 150°C (Supplementary material), there is weight loss of 7.0% with an obvious endothermal peak, corresponding to release of weakly adsorbed water, in agreement with calculated value (6.8%). Further weight loss of 13.7% is observed from 150°C to 200°C with another endothermal peak, attributed to loss of coordinated water (calculated weight loss = 13.6%). A strikingly exothermic peak at 200–400°C with weight loss of 72.1% can be ascribed to decomposition of the ligand (calculated weight loss = 70%). The exothermic peak arises due to formation of strong polar Cu–O bonds in copper oxide (end product) which compensates for rupture of covalent bonds in ligand. From 400°C to 700°C, no change in weight is found.

3.6. *N_2 TPD and BET surface area studies*

In order to determine the porosity of **1**, adsorption isotherms of nitrogen on **1** were measured at NTP. Nanosized **1** shows BET surface area of $8.6834\,m^2\,g^{-1}$ whereas single crystalline **1** developed from nanosized **1** shows BET surface area of $3.6786\,m^2\,g^{-1}$. This indicates that packing of molecules in crystalline pattern results in decrease in surface area.

Table 2. Selected bond distances (Å) and angles (°) data for **1**.

Cu(1)–N(1)	1.9087(18)
Cu(1)–O(5)	1.9706(17)
Cu(1)–O(2)	2.0098(16)
Cu(1)–O(1)	2.0099(17)
Cu(1)–O(6)	2.1564(19)
O(1)–C(8)	1.278(3)
O(4)–C(7)	1.224(3)
O(3)–C(8)	1.235(3)
O(5)–H(52)	0.76(4)
O(5)–H(51)	0.79(4)
N(1)–C(2)	1.331(3)
N(1)–C(6)	1.333(3)
O(2)–C(7)	1.285(3)
C(7)–C(6)	1.521(3)
O(6)–H(62)	0.73(3)
O(6)–H(61)	0.81(4)
C(6)–C(5)	1.381(3)
C(2)–C(3)	1.382(3)
C(2)–C(8)	1.514(3)
C(5)–C(4)	1.388(4)
C(5)–H(5)	0.95(3)
C(3)–C(4)	1.394(4)
C(3)–H(3)	0.86(3)
C(4)–H(4)	0.94(3)
N(1)–Cu(1)–O(5)	157.97(8)
N(1)–Cu(1)–O(2)	80.64(7)
O(5)–Cu(1)–O(2)	97.07(7)
N(1)–Cu(1)–O(1)	80.14(7)
O(5)–Cu(1)–O(1)	99.20(7)
O(2)–Cu(1)–O(1)	160.35(7)
N(1)–Cu(1)–O(6)	109.73(8)
O(5)–Cu(1)–O(6)	92.30(8)
O(2)–Cu(1)–O(6)	96.82(8)
O(1)–Cu(1)–O(6)	93.47(8)
C(8)–O(1)–Cu(1)	115.33(14)
Cu(1)–O(5)–H(52)	113(3)
Cu(1)–O(5)–H(51)	123(2)
H(52)–O(5)–H(51)	108(3)
C(2)–N(1)–C(6)	122.76(19)
C(2)–N(1)–Cu(1)	118.80(15)
C(6)–N(1)–Cu(1)	118.36(14)
C(7)–O(2)–Cu(1)	115.15(14)
O(4)–C(7)–O(2)	126.0(2)
O(4)–C(7)–C(6)	119.8(2)
O(2)–C(7)–C(6)	114.21(18)
Cu(1)–O(6)–H(62)	114(2)
Cu(1)–O(6)–H(61)	109(3)
H(62)–O(6)–H(61)	106(4)
N(1)–C(6)–C(5)	120.2(2)
N(1)–C(6)–C(7)	111.42(18)
C(5)–C(6)–C(7)	128.4(2)
N(1)–C(2)–C(3)	120.3(2)
N(1)–C(2)–C(8)	110.98(18)
C(3)–C(2)–C(8)	128.7(2)
O(3)–C(8)–O(1)	125.0(2)
O(3)–C(8)–C(2)	120.5(2)
O(1)–C(8)–C(2)	114.44(19)
C(6)–C(5)–C(4)	118.2(2)
C(6)–C(5)–H(5)	120.1(18)
C(4)–C(5)–H(5)	121.7(18)

(*continued*)

Table 2. Continued.

C(2)–C(3)–C(4)	117.9(2)
C(2)–C(3)–H(3)	120(2)
C(4)–C(3)–H(3)	122(2)
C(5)–C(4)–C(3)	120.6(2)
C(5)–C(4)–H(4)	121.0(17)
C(3)–C(4)–H(4)	118.4(17)

e.s.d.'s are given in parentheses.

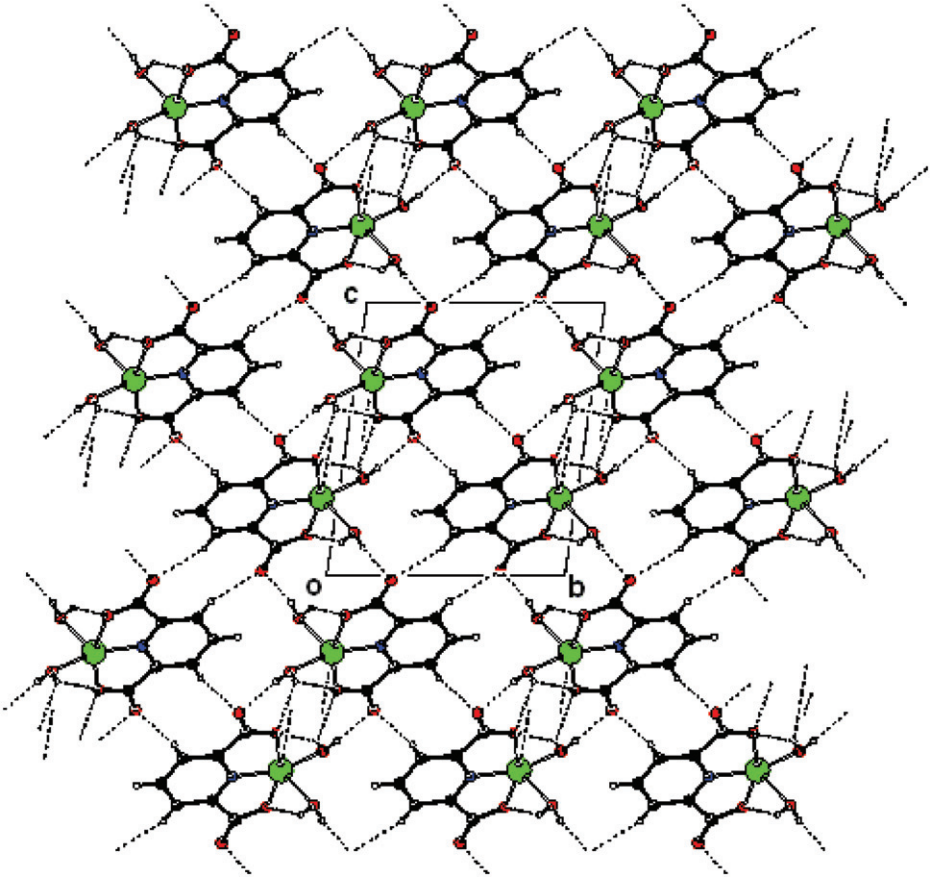

Figure 7. 3-D supramolecular arrangement of **1** when viewed along the *b*-axis. Hydrogen bonds are shown as broken lines.

4. Conclusion

A nanosized supramolecular compound, $[Cu(dipic)(H_2O)_2]_n$ (**1**), has been synthesized by sonochemical irradiation and compared with its crystalline structure, developed from the aqueous solution of nanosized compound. The crystal structure of **1** consists

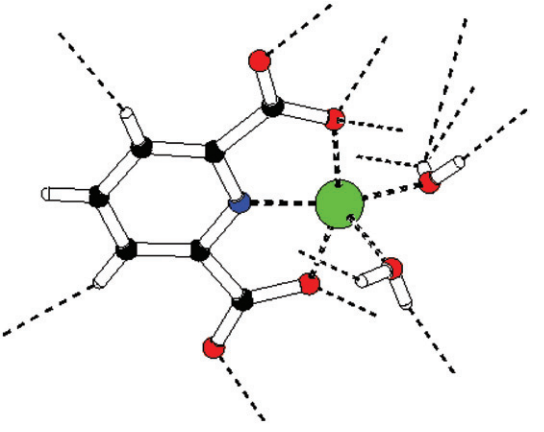

Figure 8. Number and position of hydrogen bonds of **1**. Hydrogen bonds are shown as broken lines.

Table 3. Hydrogen–bonding distance (Å) and angle (°) data for **1.**

D–H···A	D–H	H···A	D···A	D–H···A	Symmetry transformation for A
O5–H51···O3	0.77(4)	1.97(4)	2.737(3)	172(4)	$1-x, 2-y, 1-z$
O5–H52···O1	0.72(5)	2.33(5)	2.978(3)	149(5)	$-1+x, y, z$
O5–H52···O1	0.72(5)	2.49(4)	3.074(3)	140(4)	$-x, 2-y, 1-z$
O6–H61···O2	0.86(4)	2.02(4)	2.769(3)	146(4)	$1+x, y, z$
O6–H62···O4	0.75(4)	1.99(4)	2.731(3)	167(4)	$-x, 2-y, -z$
C3–H3···O3	0.87(4)	2.48(4)	3.331(3)	165(3)	$2-x, 1-y, 1-z$
C5–H5···O4	0.94(3)	2.43(3)	3.322(3)	158(3)	$-x, 1-y, -z$

e.s.d.'s are given in parentheses.

of a 3-D supramolecular network with each copper(II) coordinated to two oxygen atoms and one nitrogen atom from dipic and two oxygen atoms from coordinated water in a distorted square-pyramidal environment. Calcination of nanosized **1** produced nanoparticles of CuO, acting as a precursor for formation of nanosized CuO. Higher surface area for nanosized **1** in comparison with single crystalline **1** indicates that packing of molecules in crystalline pattern results in decrease in surface area. To prepare nanoparticles of **1**, water and a mixture of water and methanol were used as solvents. The reactions produced the same compound but with different size and morphology. Thus, solvent plays an important role in affecting the size and morphology of nanosized **1**. The mean particle size for **1** prepared in purely aqueous medium and for that prepared in mixed solvent system obtained by DLS measurements was in agreement with the data obtained from SEM images.

Acknowledgments

We gratefully acknowledge the financial support from DRDO, New Delhi. We thank the Head, Sophisticated Analytical Instrumentation Facility, Punjab University, Chandigarh for XRD and SEM.

References

[1] E. Colacio, F. Lloret, R. Kivekas, J. Ruiz, J. Suarez-Varela, M.R. Sundberg. *Chem. Commun.*, 592 (2002).
[2] G. Guilera, J.W. Steed. *Chem. Commun.*, 1563 (1999).
[3] H.W. Roesky, M. Andruh. *Coord. Chem. Rev.*, **236**, 91 (2003).
[4] M. Eddaoudi, H. Li, O.M. Yaghi. *J. Am. Chem. Soc.*, **122**, 1391 (2000).
[5] C.J. Kepert, M.J. Rosseinsky. *Chem. Commun.*, 31 (1998).
[6] C.J. Kepert, T.J. Prior, M.J. Rosseinsky. *J. Am. Chem. Soc.*, **122**, 5158 (2000).
[7] M. Kondo, M. Shimamura, S. Noro, S. Minakoshi, A. Asami, K. Seki, S. Kitagawa. *Chem. Mater.*, **12**, 1288 (2000).
[8] J.S. Seo, D. Whang, H. Lee, S.I. Jun, J. Oh, Y.J. Jeon, K. Kim. *Nature*, **404**, 982 (2000).
[9] G.T.R. Palmore, J.C. MacDonald, A. Greenberg, C.M. Breneman, J.F. Liebman. *The Amide Linkage: Structural Significance in Chemistry, Biochemistry and Materials Science*, Wiley & Sons, New York (2000).
[10] M. Hidai, O. Yaghi, H. Li, C. Davis, D. Richardson, T.L. Groy. *Acc. Chem. Res.*, **31**, 474 (1998).
[11] R. Atencio, K. Biradha, T.L. Hennigar, K.M. Poirier, K.N. Power, C.M. Seward, N.S. White, M.J. Zaworotko. *Cryst. Eng.*, **1**, 203 (1998).
[12] H. Li, C.E. Davis, T.L. Groy, D.G. Kelley, O.M. Yaghi. *J. Am. Chem. Soc.*, **120**, 2186 (1998).
[13] M. Munakata, L.P. Wu, T. Kuroda-Sowa. *Bull. Chem. Soc. Japan*, **70**, 1727 (1997).
[14] C.V.K. Sharma, R.D. Rogers. *Cryst. Eng.*, **1**, 19 (1998).
[15] O.M. Yaghi, C.E. Davis, G. Li, H. Li. *J. Am. Chem. Soc.*, **119**, 2861 (1997).
[16] T.M. Reineke, M. Eddaoudi, M. Fehr, D. Kelley, O.M. Yaghi. *J. Am. Chem. Soc.*, **121**, 1651 (1999).
[17] O.M. Yaghi, H. Li, T.L. Groy. *J. Am. Chem. Soc.*, **118**, 9096 (1996).
[18] M.G.B. Drew. *Coord. Chem. Rev.*, **24**, 179 (1977).
[19] B. Zhao, P. Cheng, Y. Dai, C. Cheng, D.Z. Liao, S.P. Yan, Z.H. Jiang, G.L. Wang. *Angew. Chem., Int. Ed. Engl.*, **42**, 934 (2003).
[20] C. Brouca-Cabarrecq, A. Fernandes, J. Jaud, J.P. Costes. *Inorg. Chim. Acta*, **332**, 54 (2002).
[21] W.-Z. Wang, X. Liu, D.-Z. Liao, Z.H. Jiang, S.P. Yan, G.L. Wang. *Inorg. Chem. Commun.*, **4**, 327 (2001).
[22] C.X. Zhang, Z.L. Liu, D.Z. Liao, Z.H. Jiang, S.P. Yan. *J. Mol. Struct.*, **650**, 21 (2003).
[23] C.X. Zhang, D.Z. Liao, Z.H. Jiang, S.P. Yan, B. Zhao. *Transition Met. Chem.*, **28**, 621 (2003).
[24] K.Y. Choi, H. Ryu, Y.M. Lim, N.D. Sung, U.S. Shin, M. Suh. *Inorg. Chem. Commun.*, **6**, 412 (2003).
[25] R. Jin, Y. Cao, C.A. Mirkin, K.L. Kelly, G.C. Schatz, J.G. Zheng. *Science*, **294**, 1901 (2001).
[26] Y.-W. Jun, J.-W. Seoa, S.J. Oh, J. Cheon. *Coord. Chem. Rev.*, **249**, 1766 (2005).
[27] F. Kim, S. Connor, H. Song, T. Kuykendall, P.D. Yang. *Angew. Chem., Int. Ed.*, **43**, 3673 (2004).
[28] S. Lv, P. Li, J. Sheng, W. Sun. *Mater. Lett.*, **61**, 4250 (2007).
[29] X. Ji, Q. Hu, J.E. Hampsey, X. Qiu, L. Gao, J. He, Y. Lu. *Chem. Mater.*, **18**, 2265 (2006).
[30] Y. Lu, H. Fan, A. Stump, T.L. Ward, T. Rieker, C.J. Brinker. *Nature*, **398**, 223 (1999).
[31] B.J.H. Bang, K.S. Suslick. *Adv. Mater.*, **22**, 1039 (2010).
[32] H. Sadeghzadeh, A. Morsali, P. Retailleau. *Polyhedron*, **29**, 925 (2010).
[33] M.A. Alavi, A. Morsali. *Ultrason. Sonochem.*, **17**, 441 (2010).
[34] F. Marandi, V. Safarifard, A. Morsali, H.-K. Fun. *J. Coord. Chem.*, **64**, 3781 (2011).
[35] B.J.H. Bang, K.S. Suslick. *J. Am. Chem. Soc.*, **129**, 2242 (2007).
[36] S. Cabanas-Polo, K.S. Suslick, A.J. Sanchez-Herencia. *Ultrason. Sonochem.*, **18**, 901 (2011).
[37] Mercury 1.4.1, Copyright Cambridge Crystallographic Data Centre, 12 Union Road, Cambridge, CB2 1EZ, UK (2001–2005).
[38] B. Ding, Y.Y. Liu, X.J. Zhao, E.C. Yang, X.G. Wang. *J. Mol. Struct.*, **920**, 248 (2009).
[39] K. Nakamoto. *Infrared and Raman Spectra of Inorganic and Coordination Compounds*, 5th Edn, Wiley & Sons, New York (1997).
[40] K. Akhbari, A. Morsali. *J. Coord. Chem.*, **64**, 3521 (2011).
[41] L. Aboutrabi, A. Morsali. *Ultrason. Sonochem.*, **18**, 407 (2011).
[42] A. Aslani, A. Morsali, V.T. Yilmaz, C. Kazak. *J. Mol. Struct.*, **929**, 187 (2009).
[43] C. Xie, Z. Zhang, X. Wang, X. Liu, G. Shen, R. Wang, D. Shen. *J. Coord. Chem.*, **57**, 1173 (2004).
[44] N. Okabe, N. Oya. *Acta Cryst.*, **C56**, 305 (2000).